Title

Transcriptomic profile analysis of brain inferior colliculus following acute hydrogen sulfide exposure

Authors

Kim, Dong-Suk
Anantharam, Poojya
Padhi, Piyush
et al.

Publication Date

2020

DOI

10.1016/j.tox.2019.152345

Peer reviewed

Published in final edited form as:

Toxicology. 2020 January 30; 430: 152345. doi:10.1016/j.tox.2019.152345.

Transcriptomic Profile Analysis of Brain Inferior Colliculus Following Acute Hydrogen Sulfide Exposure

Dong-Suk Kim[1], **Poojya Anantharam**[1,a], **Piyush Padhi**[1], **Daniel R Thedens**[2], **Ganwu Li**[1], **Ebony Gilbreath**[3], **Wilson K. Rumbeiha**[1,*]

[1]VDPAM, College of Veterinary Medicine, Iowa State University, Ames, IA

[2]Radiology, School of Medicine, University of Iowa, Iowa City, IA

[3]Department of Pathobiology, College of Veterinary Medicine Tuskegee University

Abstract

Hydrogen sulfide (H_2S) is a gaseous molecule found naturally in the environment, and as an industrial byproduct, and is known to cause acute death and induces long-term neurological disorders following acute high dose exposures. Currently, there is no drug approved for treatment of acute H_2S-induced neurotoxicity and/or neurological sequelae. Lack of a deep understanding of pathogenesis of H_2S-induced neurotoxicity has delayed the development of appropriate therapeutic drugs that target H_2S-induced neuropathology. RNA sequencing analysis was performed to elucidate the cellular and molecular mechanisms of H_2S-induced neurodegeneration, and to identify key molecular elements and pathways that contribute to H_2S-induced neurotoxicity. C57BL/6J mice were exposed by whole body inhalation to 700 ppm of H_2S for either one day, two consecutive days or 4 consecutive days. Magnetic resonance imaging (MRI) scan analyses showed H_2S exposure induced lesions in the inferior colliculus (IC) and thalamus (TH). This mechanistic study focused on the IC. RNA Sequencing analysis revealed that mice exposed once, twice, or 4 times had 283, 193 and 296 differentially expressed genes (DEG), respectively (q-value < 0.05, fold-change > 1.5). Hydrogen sulfide exposure modulated multiple biological pathways including unfolded protein response, neurotransmitters, oxidative stress, hypoxia, calcium signaling, and inflammatory response in the IC. Hydrogen sulfide exposure activated PI3K/Akt and MAPK signaling pathways. Pro-inflammatory cytokines were shown to be potential initiators of the modulated signaling pathways following H_2S exposure. Furthermore, microglia were shown to release IL-18 and astrocytes released both IL-1β and IL-18 in response to H_2S. This transcriptomic analysis data revealed complex signaling pathways involved in H_2S-induced neurotoxicity and may provide important associated mechanistic insights.

Keywords

Hydrogen Sulfide; Brain Injury; Neurodegeneration; RNA-seq analysis; Transcriptomic analysis; MRI analysis

[*]Corresponding Author's Contact Information: rumbeiha@iastate.edu, 515-294-0630.

[a]Present addresses: Poojya Anantharam: Medical Countermeasures, MRI Global, Kansas City, MO, US

The authors do not have any conflict of interest.

1. Introduction

Hydrogen sulfide (H_2S) is a flammable and colorless potent toxic gas with a “rotten egg” odor that has generally been considered as an environmental hazard (Chou et al. 2016). However, recently it has been shown that H_2S is endogenously produced in low concentrations in multiple organs including heart, brain, kidney, and aorta (Olas 2014). In low physiological concentrations H_2S plays important roles including acting as a gasotransmitter, regulating vascular tone (Lavu et al. 2011), serving as an anti-inflammatory compound (Lavu et al. 2011), and as a scavenger of reactive oxygen species (ROS) (Lavu et al. 2011). It also plays a beneficial role in several diseases including cancer (Lee et al. 2011) and Parkinson’s disease (Hu et al. 2010). Hydrogen sulfide has also been shown to be involved in multiple signaling pathways including protein kinase A, mitogen and receptor tyrosine kinases, oxidative stress, calcium channels and neurotransmission, among others (Tan et al. 2010).

Acute exposure to high concentrations of H_2S induces concentration-, time- and dose-dependent toxicity in humans and animals (Anantharam et al. 2017; Board 2004; Rumbeiha et al. 2016). It is the second most common cause of acute toxic gas induced mortality, after carbon monoxide (Greenberg and Hamilton 1998). Acute exposure to 30 ppm H_2S induces olfactory fatigue and malfunction of the nose. At concentrations higher than 500 ppm H_2S induces headache, dizziness and respiratory failure. Additional effects of H_2S concentrations > 500 ppm include respiratory paralysis, seizures, and loss of consciousness (knock-down). A brief exposure to H_2S > 1000 ppm can be instantly fatal. Environmental H_2S is released naturally from volcanoes, sulfur springs, stagnant water bodies and geothermally active areas. Hydrogen sulfide can also be produced by human activities such as desulfurization processes in oil and gas industries, paper mills, manure treatment facilities, and in water purification facilities. It is a toxic industrial raw chemical material. Hydrogen sulfide can easily be generated from mixing simple raw materials and has been used for suicide purposes (Sams et al. 2013). In addition, H_2S can potentially be used for nefarious activities by terrorists (National Institute of Allergy and Infectious Diseases 2007; Ng et al. 2019); therefore, potential misuse of this potent toxicant by terrorists is concerning and a major risk to victims and first responders (Ng et al. 2019; Sams et al. 2013). Survivors of acute exposure to high concentrations of H_2S may manifest one or more neurological deficits including slurred speech, memory loss, dizziness, sleep disturbances, depression, delirium, altered psychological states, spasms, and motor dysfunction (Board 2004; Chou et al. 2016; Guidotti 2010; Guidotti 2015; Kilburn 2003; Matsuo et al. 1979; Parra et al. 1991; Rumbeiha et al. 2016; Tvedt et al. 1991a; Tvedt et al. 1991b; Wasch et al. 1989). There are more than 1,000 annual reports related to severe H_2S exposure in the Unites States (U.S. Department of Health and Human Services 2014). Despite the high mortality and morbidity of acute H_2S poisoning, there is no suitable antidote available for field use to treat civilian casualties and to prevent development of incapacitating neurological sequelae.

The exact molecular and cellular mechanisms behind H_2S-induced neurological disorders are poorly understood and this is the main reason responsible for delayed development of drugs for treatment of H_2S-induced acute toxicity, though a few toxic mechanisms have been suggested. For example, cytochrome c dependent apoptosis with DNA damage was

previously reported to play a role in H_2S-induced neurotoxicity (Kurokawa et al. 2011). Glutamate-induced cytotoxicity was also reported to be involved in H_2S exposure-induced neurotoxicity (Cheung et al. 2007; Garcia-Bereguiain et al. 2008). Reduction of glutathione (GSH), an antioxidant, and generation of ROS have also been shown to play a role *in vitro* (Truong et al. 2006). Most of these studies were done *in vitro* and have not been confirmed in *in vivo* animal models. There is still a wide knowledge gap in understanding the mechanisms of H_2S-induced neurotoxicity. Closing this gap is critical for the development of novel therapeutic antidotes.

In this study, we used a relevant inhalation mouse model of H_2S-induced neurotoxicity developed in-house to study molecular mechanisms of acute H_2S-induced neurotoxicity using transcriptomic analysis. This mouse model manifests motor and behavioral deficits, respiratory depression, seizures, and knock-down, recapitulating the human condition (Anantharam et al. 2017). In this study, we have shown that magnetic resonance imaging (MRI) analysis from live mice exposed to H_2S revealed neurodegeneration in the inferior colliculus (IC) and in the thalamus (TH). We focused on the neurodegeneration in the IC, the most severely affected region, and showed that transcriptomic analyses of the IC of mice acutely exposed to H_2S had multiple modulated biological pathways and potential upstream regulators. Among these, the PI3K/Akt and MAPK signaling pathways were activated following acute H_2S exposure. We showed that microglia and astrocytes released the pro-inflammatory cytokines, IL-1β and IL-18. This data provides valuable information on molecular targets which may play an important role in the development of novel antidotes or therapies for acute H_2S-induced neurotoxicity.

2. Materials and Methods

2.1 Chemicals

Hydrogen sulfide gas [CAS 7783-06-4] was purchased from Airgas (Radnor, PA). RNeasy mini kit was purchased from Qiagen (Germantown, MD). High Capacity cDNA RT kit were purchased from ThermoFisher Scientific (Waltham, MA). RT² SYBR Green ROX qPCR Mastermix and primers for Gapdh were purchased from Qiagen (Valencia, CA).

2.2 Animals

All animal studies were approved by the Iowa State University Institutional Animal Care and Use Committee (IACUC). Animals were cared for in accordance with IACUC guidelines. Mice were purchased from Jackson Laboratories (Bar Harbor, ME). Seven-to eight-week-old male C57 BL/6J mice were housed at room temperature (RT) of 20 – 22 °C under a 12-h light cycle, and a relative humidity of 35 – 50 %. Protein Rodent maintenance diet (Teklad HSD Inc, WI, US) and water were provided *ad libitum*. All mice were acclimated to breathing air for 1 week before H_2S exposure. We chose to use the C57BL/6J mouse model because it is widely used for neurodegenerative research. This model has effectively recapitulated H_2S-induced neuropathology in our hands (Anantharam et al. 2018a; Anantharam et al. 2017). In this study, we used male mice only because, as previously reported, male mice were more sensitive than female mice (Anantharam et al. 2018a; Anantharam et al. 2017).

2.3 Transcriptomic analysis

2.3.1 Exposure paradigm—For transcriptomic analysis, mice were exposed to H_2S either once, twice or 4 times. Mice exposed once reflect the typical human accidental exposure scenario. Mice exposed 2 or 4 times were used for comparison to the typical one-time exposure. Mice were exposed by whole body inhalation either to normal breathing air from a tank (Control) or to 700ppm H_2S for 40 min on day 1 for mice which received one exposure. For mice which received 2 exposures, they were exposed to 700ppm H_2S for 40 min on day 1 and for 15 min on day 2. For mice which received 4 exposures they received 700ppm H_2S for 40 min on day 1 and for 15 mins per day on subsequent days up to day 4 (Fig. 1). Control group mice were exposed to breathing air daily for 4 days. We chose this H_2S exposure level of 700 ppm because we are mimicking high dose exposures as would be encountered during terrorism incidents or accidents in which concentrations of H_2S exceed 500 ppm. The duration of exposure in field accidents can vary depending on how quickly first responders get to the site, terrain, etc. For our studies, exposure duration was based on preliminary dose-response and time course studies (Anantharam et al. 2017). Following rapid decapitation, brains were immediately removed from the skull. The IC of the four mice in each group were microdissected on ice and immediately flash frozen using liquid nitrogen and stored at −80°C until further use.

2.3.2 RNA isolation—Total RNA was extracted from frozen tissues using the RNeasy® Plus Mini kit with treatment of DNase I according to the manufacturer's protocol (Qiagen, Germantown, MD). The integrity of RNA samples were examined by running on agarose gel and using bioanalyzer.

2.3.3 Transcriptome profiling with RNA-Seq—Construction of library of samples was followed by TruSeq® RNA Sample Preparation v2 Guide (Illumina). Briefly, poly (A) -containing mRNA of samples were used for first-strand cDNA synthesis using Super Script II (Invitrogen). RNA Index adapter were ligated to the cDNA products, followed by several rounds of PCR amplification. The resulting libraries of samples were sequenced using HiSeq 2000 System (Illumina). The library construction and RNA-Seq were performed at BGI America (Cambridge, MA).

2.3.4 Transcriptome analysis—Transcriptomic profiling was processed following Tuxedo protocol (nature paper) with slight modification. For the modifications, we used STAR software for mapping raw data to the mouse reference genome (GRCm38.p4 downloaded from https://www.gencodegenes.org/mouse/release_M11.html). STAR (version 2.5.1), samtools (version 0.1.19), Bowtie 2 (version 2.2.7), cufflinks (version 2.2.1), tophat 2 (version 2.1.0) were used for the analyses. Differentially expressed genes (DEG) were obtained by using cuffdiff, part of Tuxedo suite software. Ingenuity Pathway Analysis (Qiagen) was used to analyze gene ontology analyses including altered biological pathways and potential initiator. DEGs common in immediate, early, and late response were used to generate heat map by using R software (version 3. 3. 2, https://cran.r-project.org). Ingenuity Pathway Analysis software (Qiagen, Germantown, MD) was used for dysregulated biological pathway and potential upstream regulator analysis.

2.3.5 Validation of gene expression via quantitative real-time RT-PCR—

Total RNAs were extracted from frozen tissues using the RNeasy® Plus Mini kit and treated with DNase I (Invitrogen) according to the manufacturer's protocol. cDNA was prepared using High-Capacity cDNA Reverse Transcription Kits from ThermoFisher Scientific (Waltham, MA). RT^2 SYBR Green ROX qPCR Mastermix and primers for Gapdh were purchased from Qiagen (Valencia, CA). The threshold cycle (C_t) was calculated from the instrument software, and fold change in gene expression was calculated using the $\Delta\Delta C_t$ method as described earlier (Kim et al. 2016). Primer sequences will be provided upon request.

2.4 Western blot analysis

For Western blot analysis mice were exposed to H_2S once a day for up to 7 days. Mice were exposed to 700ppm H_2S for 40 min on day 1 (single exposure) or to 700ppm H_2S for 40 min on day 1 and for 15 min per day on subsequent days up to day 7 (2 to 7 exposures). Control group mice were exposed to breathing air from a tank daily for 7 days (Fig. 4). Following rapid decapitation, brains were immediately removed from the skull. The IC of three mice in each group were microdissected on ice and immediately flash frozen using liquid nitrogen and stored at −80°C until further use. Samples were lysed with modified RIPA lysis buffer 1% Triton X-100, 1 mM EDTA, 100 mM NaCl, 1 mM EGTA, 1 mM NaF, 20 mM $Na_4P_2O_7$, 2 mM Na_3VO_4, 10% glycerol, 0.1% SDS, 0.5% deoxycholate, 50 mM Tris-HCl, and pH 7.4) via sonication, followed by centrifugation as described previously (Kim et al. 2016). Briefly, the samples containing equal amounts of proteins were loaded and fractionated in SDS-PAGE gel and transferred onto a nitrocellulose membrane overnight at 4°C. Membranes were blocked with 5% bovine serum albumin in TBS supplemented with 0.1 % Tween-20. Primary antibodies against specific proteins were incubated with the membrane overnight at 4°C.

The antibodies detecting phosphorylated proteins were purchased from Cell Signaling Technology (Cell Signaling Technology, Danvers, MA). Primary antibodies against PKA Cα, PI3K and pan-Akt were purchased from Cell signaling (Cell Signaling Technology, Danvers, MA). Primary antibodies against ATF2, and CREB-1 were purchased from Santa Cruz Biotechnology (Santa Cruz Biochnoloby, Dallas, Tx). After rinsing thoroughly in PBS supplemented with 0.1% Tween-20, the membrane was incubated with secondary antibodies. For the loading control, β-actin antibody was used. Immunoblot imaging was performed with an Odyssey Infrared Imaging system (LI-COR, Lincoln, NE). ImageJ software (National Institutes of Health, Bethesda, MD) was used to quantify Western blot bands of targeted proteins.

2.5 Magnetic resonance imaging analysis

For proof-of-principle, mice for MRI analysis were exposed by whole body inhalation either to normal breathing air from a tank (Control) or to 700ppm H_2S for 40 min on day 1 and for 15 min per day on the subsequent 6 days (Fig. 6). Five mice in each group were transported to University of Iowa where MRI scanning was performed. MRI was performed using a Discovery MR901 7T small animal imager (GE Healthcare) at the University of Iowa, Iowa City, IA. Mice were anesthetized with isoflurane (3% in an induction followed by 1.5% via a nose cone for maintenance at 0.8 l/min flow rate in oxygen). Mice were kept warm during

imaging. For T2 weighted imaging of the whole brain, a fast spin echo sequence was used (TR = 9100 ms, TE = 80 ms, matrix 256 × 192, number of slices = 40, field of view = 2.5 × 1.9 cm, slice thickness = 0.4 mm, 12 echoes, echo spacing = 8.9 ms, number of averages = 10, total acquisition time approximately 18 min). Brain lesion sizes were quantified using ImageJ software (NIH) by measuring the area of lesions.

2.6 Cell culture and quantitative RT-PCR for inflammatory response analysis

Mouse microglial cells, MMC, were kindly gifted from Dr. Anumantha Kanthasamy (Iowa State University, Ames, IA). MMC cells have been shown to mimic neonatal primary mouse microglia and to be a good mouse microglia model for neurotoxicity study (Sarkar et al. 2018b). U373 are established astrocytoid cells from human astrocytoma cell line and are suitable for neurotoxicity studies (Sarkar et al. 2018a). U373 and MMC were maintained in DMEM/F-12 media supplemented with 10% fetal bovine serum, 2 mM L-glutamine, 50 units of penicillin, and 50 μg/ml of streptomycin in a humidified incubator with 5% CO_2 at 37°C as described previously (Kim et al. 2017). Cells were seeded to confluent at 50% next day. Cells were exposed to 1 mM of Sodium hydrosulfide (NaHS) [CAS 16721-80-5] for 6 h before harvesting total RNA. Total RNAs were used to produce cDNA for quantitative RT-PCR.

2.7 Statistical analysis

Data were analyzed using Prism 4.0 (GraphPad Software, San Diego, CA). Non-paired Student's *t*-test was used when two groups were being compared. Differences were considered statistically significant at p-values <0.05. Data are represented as the mean ± S.E.M. of at least two separate experiments performed at least in triplicate.

3. Results

3.1 Acute exposure to H_2S induced brain lesions in thalamus and inferior colliculus in C57 black mice.

A previous study of ours revealed that H_2S exposure induced overt necrosis most consistently in the IC (Anantharam et al. 2017). It is for this reason that we chose to study the IC in this experiment. In this study, we sought transcriptomic profiling analyses in the IC of H_2S-exposed mice to search for key molecules involved in H_2S-induced neurotoxicity at various time points as previously described (Fig. 1). Immediate response was measured at 2 h post a single H_2S exposure. Early response was measured at 26 h post H_2S exposure (mice were subjected to 2 acute H_2S exposures 24 hrs apart and euthanized 2 h after the second exposure). The late response was measured following 4 days of acute H_2S exposure. Mice exposed to H_2S showed motor-behavioral deficits, respiratory depression, seizures and knock-down phenotype as previously reported ((Anantharam et al. 2017; Kim et al. 2018b)).

3.2 H_2S exposure induced altered transcriptomic profiling in the IC

The IC was used for transcriptomic profiling analysis because it is one of the two most sensitive brain region following acute H_2S exposure following the exposure paradigm used in this study. Transcriptomic profiling analyses of the IC were performed at 2 h, day 2, and day 4 after H_2S exposure (see Fig. 1A) following Tuxedo protocol (Trapnell et al. 2012).

The numbers of significantly up-regulated and down-regulated genes are shown in the Venn diagram (Fig 1B). 171, 142, and 247 genes were upregulated after H_2S exposure, respectively at 2h, 26h, and 4 days, respectively. 112, 51, and 49 genes were downregulated following H_2S exposure, at 2 h, 26 h, and 4 days, respectively. The genes that are up-regulated and down-regulated in common at all three time points are shown in the heatmap in Fig. 2.

3.3 H_2S exposure caused dysregulation of molecular biological pathways in the IC

Differentially expressed genes were used to analyze the dysregulated molecular biological pathways in the IC following H_2S exposure. The top 10 dysregulated pathways are listed in table 1. Results show that a single H_2S exposure and two acute H_2S exposures shared many common altered pathways including unfolded protein response, coagulation system, and NRF2-mediated oxidative stress responses. A single H_2S exposure by itself induced multiple dysregulated biological pathways (Table 1). In contrast, 4 days of repeated daily H_2S exposures induced inflammation-related pathways (Table 1). The top 10 potential upstream regulators were also analyzed (table 2) for each time point. Note that factors related to initiation of the inflammatory response were found to be common throughout the study period, including 2 hrs following a single exposure (immediate response) (Table 1).

3.4 Validation of gene expression profiles using quantitative real-time PCR

Quantitative real-time PCR of selected genes was performed to validate the gene expression profiles in the IC. Results show that genes that were significantly differentially expressed were shown to have similar trends with results of quantitative real-time PCR (Fig. 3). Selected genes that were differentially expressed in common throughout H_2S exposure are shown in Fig. 3.

3.5 H_2S exposure induces activation of PI3K/Akt signaling pathway

Akt plays an important role in cell proliferation, cell death, and many other functions (Los et al. 2009) and mediates multiple signaling pathways including calcium signaling, JNK pathway, GABA signaling, mTOR signaling and cell death signaling which were all shown to be dysregulated by acute H_2S exposure (Table 1). Phosphorylation of Akt at threonine 308 and at Serine 473 was increased by more than two fold at 2h following a single acute H_2S exposure and 26 h post H_2S exposure [2 h following a second acute H_2S exposure], indicating activation of Akt (Fig. 4). Expression of phosphoinositide 3-kinases (PI3K) also followed a similar trend following H_2S exposure (Fig. 4). These results show that exposure to H_2S may activate the PI3K/Akt signaling pathway. Phosphorylation of cAMP-dependent protein kinase (PKA) shares substrate specificity with Akt. C subunit of PKA at Thr 197 was increased in the early phase of H_2S exposure (Fig 4). Akt activates many substrates downstream in the signaling cascade. P70 S6 kinase, one of downstream substrates of Akt signaling, was phosphorylated at Thr 389 at 2h following a single acute H_2S exposure.

3.6 H_2S exposure induced activation of the MAPK signaling pathway

Mitogen-activated kinases (MAPKs) transduce and amplify extracellular stimuli into a wide variety of cellular responses (Kamiyama et al. 2015). MAPKs signaling pathway also

interacts with the PI3K/Akt signaling pathway (Lee et al. 2006; Pappalardo et al. 2016). Activation of MAPKs signaling pathway during acute H_2S exposure was evaluated in the IC. Phosphorylation of stress-activated protein kinase (SAPK) was increased more than three-fold during the immediate and early phases of acute H_2S exposure (Fig 5). Phosphorylation of p38 MAPK at Thr 180 / Tyr 182 was increased more than four-fold (Fig 5). However, ERK1/2 expressions were not altered during H_2S exposure (data not shown). Nonetheless, the expression of the activating transcription factor 2 (ATF2), one of the downstream substrates of p38 MAPK and SAPK, was increased during the early and late phases of H_2S exposure (Fig 5). Expression of cAMP responsive binding protein 1 (CREB-1), another downstream substrate of SAPK signaling pathway, was also increased after H_2S exposure (Fig 5). Expression of Fos and JunB were shown to be increased at the transcription level (Fig 3).

3.7 MRI revealed injury of the IC and thalamus following acute H_2S exposure

Previously, we reported that H_2S exposure induced histological lesions in the IC and TH (Anantharam et al. 2017). To evaluate brain lesions following acute H_2S exposure *in vivo*, the entire brains of live mice were scanned by coronal MRI. MRI analyses revealed hyperintense lesions in the IC and thalamus (TH) of H_2S-exposed mice compared to breathing air control group, suggesting severe edema in these regions (Fig. 6 B). Results of lesion size are summarized in Fig. 6 C. No lesions were found in the IC and TH of control mice exposed to breathing air.

3.7 H_2S exposure induced production of pro-inflammatory cytokines in immune cells *in vitro*

The late phase of H_2S exposure was shown to involve many biological pathways related to inflammation. To identify the cell types involved in the inflammatory response in acute H_2S-induced neurotoxicity, astrocyte and microglial cells were tested *in vitro*. MMC and U373 human astrocyte cells were exposed to 1mM NaHS, a chemical H_2S donor, for 6h. IL-1β was upregulated in both microglial and astrocyte cells, while IL-18 was upregulated in microglial cells (Fig 7).

4. Discussion

Acute exposure to high concentration of H_2S induces detrimental neurotoxic effects including seizures, knockdown, respiratory depression, and sudden death in animals. The exact mechanisms of H_2S-induced neurotoxicity have not been elucidated yet, which has delayed the development of appropriate antidotes/therapies for treatment of H_2S-induced neurotoxicity.

In this study we used the inhalational animal model of acute H_2S toxicity developed in our lab (Anantharam et al. 2017) to assess transcriptomic analysis in the IC to identify key molecules playing important roles in the pathogenesis of H_2S-induced neurotoxicity. A single and repeated acute exposure paradigm was used in this study, which emulates reported accidents with multiple exposure to high doses of H_2S (Ahlborg 1951), although a single exposure is a more common accidental scenario. The exposure paradigm in this study

also allows comparative effects of repeated acute exposures to a single exposure. Thus, this experimental design allowed exploration of acute H_2S-toxicity outcomes from immediate response (same day following single acute exposure) to late response to H_2S exposure (following repeated short acute exposures). Transcriptomic profiling analyses showed that H_2S exposure significantly induced DEG profiling involving multiple dysregulated biological pathways, even following a single acute exposure.

One phenotype of H_2S intoxication is seizure activity. Seizure activity can be induced by dysregulation of neurotransmitters in the central nervous system (CNS). Previous work from our laboratory has shown that acute H_2S exposure increases brain dopamine and serotonin concentrations (Anantharam et al. 2017). In this study, catecholamine biosynthesis was suppressed as there was downregulation of dopamine beta-hydrolyxase (Dbh), dopa decaboxylase (Ddc), and tyrosine hydroxylase (Th) 2h following a single acute H_2S exposure. The increased level of dopamine following acute H_2S exposure may suppress the expression of genes of dopamine synthesis pathway. The transcriptomic profiling analysis also revealed that gamma-aminobutyric acid (GABA) signaling pathway was dysregulated at the immediate (single exposure) and early response phases 2 h after the second dose of acute H_2S exposure. GABA transporters including solute carrier family 6 member 12 and solute carrier family 6 member 13 were upregulated at the immediate response phase (2 h after a single acute H_2S exposure). Several GABA receptor subunits including GABA type A receptor alpha6 subunit and GABA type A receptor rho2 subunit were also upregulated in the early response phase. Previous work showed an increase of the glutamate:GABA ratio following H_2S exposure (Anantharam et al. 2017). The decreased level of GABA as seen in previous studies may have induced an increase in the expression of the genes involved in GABA regulation to compensate for the deficit of GABA levels. Previously we have shown that suppression of seizure activity by treatment with an anti-convulsant drug, midazolam (MDZ), significantly rescued mice from death (Anantharam et al. 2018a). It is plausible that the effects of MDZ may have lessened the harmful effects of glutamate signaling cascade by augmenting GABA signaling cascade. Cysteine rich with EGF-like domains 2 (Creld2) may regulate transport of α4-β2 neuronal acetylcholine receptor. Creld2 was down-regulated, indicating suppression of acetylcholine signaling pathways during H_2S exposure. These results indicate H_2S exposure may mediate dysregulation of multiple neurotransmitter signaling pathways and this may play important roles in H_2S-induced neurotoxicity in the IC. All these changes in neurotransmitter patterns likely contribute to H_2S-induced seizures. More work remains to be done to piece together which of these changes play dominant roles in seizure induction.

Hydrogen sulfide is well known to induce vasodilation (Lavu et al. 2011). Endothelin1 (Edn1) works as an endothelium-derived vasoconstrictor. Edn1 was consistently upregulated more than two folds after H_2S exposure. In addition, genes associated with activation of coagulation system were upregulated. Specifically, coagulation factor III (F3), plasminogen activator tissue type (Plat), plasminogen activator urokinase receptor (Plaur), and serpin family E member 1 (Serpine1) were all upregulated 2 h following a single acute H_2S exposure, suggesting blood vessel injury and brain hemorrhage. F3, plat, and plaur were upregulated 2 h after a single acute H_2S exposure and after two acute exposures (early response), while alpha-2-macroglobulin (A2m) and von Willebrand factor (Vwf) were

upregulated from early response (2 exposures to H_2S) to late response (4 exposures to H_2S). These results further support our previous findings that H_2S exposure may induce hemorrhage in the IC, suggesting a breach of the blood brain barrier may play a role in H_2S-induced neurotoxicity (Kim et al. 2018a). Considering that the IC requires high blood supply for playing a role as a hub for hearing (Huffman and Henson 1990), this region has a dense blood capillary network. We postulate that H_2S-induced blood vessel injury and subsequent hemorrhage in the IC may also contribute to hypoxic conditions in the IC.

We have previously shown that H_2S exposure activated the hypoxic signaling pathway and upregulated Hif-1α (Kim et al. 2018a). The Akt signaling pathway has previously been shown to be activated under hypoxic conditions and reportedly plays an important role in survival of neuronal cells (Alvarez-Tejado et al. 2001); it also mediates the Hif-1α signaling pathway (Kilic-Eren et al. 2013). Transcriptomic analysis revealed H_2S exposure induced activation of Akt signaling pathway at the immediate and early phases. Concomitantly, PI3K was significantly upregulated at the immediate and early response phases. In addition, PKA was also activated at the immediate and early phases following acute H_2S exposure. p70 S6K, one of substrates of Akt signaling pathway, was also activated immediately at the immediate phase following acute H_2S exposure. Collectively, this data indicates that H_2S exposure induced hypoxic conditions in the IC which then activated the Akt pathway for the survival of neuronal cells in the IC.

This study also provided more evidence on the involvement of oxidative stress in the pathogenesis of acute H_2S-exposure. Hydrogen sulfide exposure consistently induced oxidative stress response in the IC throughout the course of this study, starting from 2 h following a single acute exposure (immediate) to following 4 exposures (late response). Impairment of cytochrome c oxidase by ethanol overdose was previously reported to generate ROS (Srinivasan and Avadhani 2012). Hydrogen sulfide may generate ROS by inhibiting cytochrome c oxidase in a similar manner. In our previous studies we have demonstrated that H_2S-inhibits cytochrome c oxidase (Anantharam et al. 2017); moreover, H_2S exposure also led to the generation of hydroxyl radicals (Jiang et al. 2016) all of which contribute to oxidative stress. In our previous work, we have reported that H_2S exposure activated the Nrf2 signaling pathway (Kim et al. 2018a), further supporting the hypothesis of H_2S-induced oxidative stress as a toxic mechanism. MAF BZIP transcription factor F (Maff) is a basic leucine zipper transcription factor and forms a heterodimer with Nrf2 to induce antioxidant or electrophile response elements (AREs) (Katsuoka et al. 2005). In this study we have shown that H_2S exposure consistently induced upregulation of Maff and Mafk following H_2S exposure. Uncoupling protein 2 (Ucp2) is a mitochondrial transporter protein and was shown to be upregulated 70 – 100% after H_2S exposure in the IC compared to breathing air control group. Ucp2 creates proton leakage across the inner mitochondrial membrane to uncouple oxidative phosphorylation from ATP synthesis, which plays a role in controlling ROS production (Mailloux and Harper 2011) and in calcium regulation (Motloch et al. 2016). Collectively, these data further show that H_2S exposure induces significant oxidative stress. Thus therapies targeting inhibition of H_2S-induced oxidative stress may be good candidates for treating H_2S-induced neurotoxicity.

Hydrogen sulfide exposure induced dysregulation of the calcium signaling pathway in this study, indicating intracellular calcium may be dysregulated. It is reported that H_2S exposure increased intracellular Ca^{2+} concentration via PKA and PLC/PKC pathways (Yong et al. 2010). Hydrogen sulfide exposure indeed activated PKA by phosphorylation at T197 in this study. Multiple factors such as impaired cytochrome c oxidase activity with subsequent reduced energy production, oxidative stress, and Ca^{2+} dysregulation may collectively induce endoplasmic reticulum (ER) stress, leading to unfolded protein response which we observed in this study. Nonetheless, further research is required to examine how H_2S exposure exactly induces the unfolded protein response. However, RNA Seq analyses in this study revealed several heat shock protein family genes were downregulated after H_2S exposure including HSPA1b, HSPA2, HSPA5, HSPA1A. HSPA5 encodes the binding immunoglobulin protein which serves an important role in ER stress (Wang et al. 2017). Hydrogen sulfide exposure also downregulated X-Box binding protein 1 (Xbp1). Xbp1 plays an important role in unfolded protein response (UPR) (Bahar et al. 2016). Interestingly, Mitogen-activated protein kinase 6 (Map3k6) was upregulated in the IC of H_2S exposed mice more than two to three folds. Apoptosis signaling kinase 1 (Ask1) responds to ER stress and induces JNK activation (Hattori et al. 2009). Map3k6 functions to activate Ask1 by phosphorylation. Indeed, acute H_2S exposure activated JNK and p38 signaling pathways. Several Jun proteins including Jun proto-oncogene (Jun), Jun B proto-oncogene (JunB), and jun D proto-oncogene (JunD) were also consistently upregulated after H_2S exposure following either a single exposure (immediate), two exposures (early), and 4 exposures (late). Collectively, this data implicates the endoplasmic stress and unfolded protein response as a potential key mechanism leading to cell death following exposure to acute H_2S poisoning. It may be worthy to explore targeting this pathway as a potential therapeutic approach for treatment of acute H_2S-induced neurotoxicity.

The cell death signaling pathway was dysregulated 2 h following a single acute exposure to H_2S. For example, expression of the anti-apoptotic gene, Bcl-2, was downregulated 2 h after a single H_2S exposure. p53 signaling pathway which senses DNA damage was also activated at 2 h following a single acute H_2S exposure. Cyclin D2 (Ccnd2), cycline-dependent kinase inhibitor 1A (Cdkn1a), growth arrest and DNA damage inducible gamma (Gadd45g), tumor protein p53 inducible nuclear protein 1 (Trp53inp1), and Fas were also upregulated 2 h following a single acute exposure to H_2S (immediate response), indicating early activation of the p53 signaling pathway. Fat atypical cadherin 2 (Fat2) is a tumor suppressor gene which plays a role in controlling cell proliferation (Katoh 2012). Expression of Fat2 was consistently upregulated following H_2S exposure indicating that cell death signaling was activated. Cd93 is a cell-surface glycoprotein and was shown to be involved in intercellular adhesion and in the clearance of apoptotic cells. Consistent upregulation of Cd93 following H_2S exposure may indicate that H_2S exposure induced cell death during H_2S exposure. However, NFkB inhibitor, alpha (Nfkbia), was consistently upregulated, while Tumor Necrosis Factor (Ligand) Superfamily, Member 10 (Tnfsf10) was consistently downregulated. Collectively, several cell survival and cell death signaling pathways were involved in H_2S exposure response. The meaning of all these changes is not clear from this one study. Clearly, a better understanding of cell survival and death signaling pathways in detail requires further studies.

To gain insight of brain pathology in live H_2S exposed mice, non-invasive MRI scanning imaging system was used. T2 weighted imaging showed edema in the IC and TH of mice indicating significant neurodegeneration in these two brain regions on day 8 following H_2S exposure. These MRI results are consistent with our previous histology and immunohistochemistry results (Anantharam et al. 2017; Kim et al. 2018a) which showed that H_2S exposure induced severe loss of neurons and activation of neuroinflammation starting on day 3. Both the IC and TH have been linked to seizures. The origin of H_2S-induced seizure is yet to be determined. The IC is a part of the brain stem which serves as a major auditory center in the brain. Interestingly, the IC has been linked to audiogenic seizure (Garcia-Cairasco et al. 1996). GABA plays an important inhibitory role whereas glutamate-mediated stimulation is excitatory to neurons in the IC (Faingold 2002). The TH has also been linked to different forms of seizures including absence seizure, temporal lobe seizures and generalized seizures (Carney and Jackson 2014). We previously showed that pre-treatment of mice with MDZ, an anticonvulsant agent, protected mice from H_2S-induced seizures and death (Anantharam et al. 2018b). Midazolam pretreatment also significantly reduced lesion severity in these two regions. This data suggests that seizures play important roles in H_2S-induced neurotoxicity, cell death, and evolution of neurological sequalae. In other words, seizures may be linked to the development of lesions both in the IC and the TH since pretreatment with midazolam significantly reduces lesion severity in both regions.

The analysis for potential upstream regulator(s) after H_2S exposure revealed an inflammatory response (e.g. TNFα, IL-1β, and IL-6) in addition to transcription factors for cell proliferation and death, such as p53, in all phases of H_2S-induced neurotoxicity examined in this study. These data indicate that the H_2S exposure immediately induces a pro-inflammatory response as IL-1β was upregulated immediately following acute H_2S exposure. IL-1β, IL-18, IL-6, Ccl2, and TNF-α were all upregulated in IC during the early and late phases after H_2S exposure. *In vitro* cell culture studies further showed that mouse microglial cells produce IL-1β and IL-18, while human astrocytes cells produce IL-18 at 6h in response to H_2S exposure. Previously we have shown that glial fibrillary acidic protein (GFAP) was upregulated by acute H_2S exposure (Anantharam et al. 2017). Collectively, these data show that microglia and astrocytes immediately respond to H_2S exposure and elicit initial neuro-inflammatory reactions. In turn, these reactions unleash powerful neuroinflammation with production of Ccl2, TNF-α, and IL-6 leading to neuronal loss and neurodegeneration in the IC (Anantharam et al. 2017). The implication of these results is that drugs which suppress neuro-inflammation may be potential candidates for counteracting H_2S-induced neuroinflammation.

5. Conclusions

In the past, the mechanisms of H_2S-induced neurotoxicity and neurodegeneration have remained poorly understood. In this study, we performed transcriptomic analysis of the IC in mice following acute H_2S exposure. Results revealed important key molecules and molecular pathways including unfolded protein response, neurotransmitters, calcium dysregulation, oxidative stress, survival/death, hypoxia, and inflammatory response in the IC following acute H_2S exposure. Potential upstream regulators in IC were found to be inflammatory initiators such as TNF, IL-1β and IL-18. These results are consistent with

some of the previous findings which we have published. This study has also proved that *in vivo* MRI analysis is effective in imaging the lesions in IC and TH following H_2S exposure. *In vitro* studies showed that microglia and astrocytes released IL-1β and IL-18 which we hypothesized to be key molecules in orchestrating multiple biological pathways. The overall hypothetical schemes of key events are presented in Figs 8 and 9. Overall, this novel study has shown that multiple complex biological pathways are involved in the pathogenesis of H_2S-induced neurotoxicity. The common simplistic dogma that H_2S-induced neurotoxicity is caused by inhibition of cytochrome c oxidase leading to energy deficit and cell death should be critically questioned and explored while also examining other mechanistic pathways. More research is warranted to further define the exact molecular mechanisms involved in H_2S-induced neurotoxicity. Collectively, this study has identified important key elements, biological pathways, and potential signal cascade initiators involved in H_2S-induced neurotoxicity and the evolution of neurological sequelae. More in-depth research is needed to further define the pathways leading to neuronal cell death and more definitive therapeutic targets.

Acknowledgment:

This work was supported by Iowa State University College of Veterinary Medicine Seed grant and Iowa State University Tuskegee Collaboration Seed grant. None of the funder played a role in any of the studies presented in this manuscript.

Abbreviations:

H_2S	hydrogen sulfide
IC	inferior colliculus
TH	thalamus
MRI	Magnetic resonance imaging
DEG	differentially expressed genes
ROS	reactive oxygen species
IL	interleukin
NaHS	Sodium hydrosulfide

References

Ahlborg G 1951. Hydrogen sulfide poisoning in shale oil industry. A.M.A. archives of industrial hygiene and occupational medicine 3, 247–266. [PubMed: 14810252]

Alvarez-Tejado M, Naranjo-Suarez S, Jimenez C, Carrera AC, Landazuri MO and del Peso L 2001. Hypoxia induces the activation of the phosphatidylinositol 3-kinase/Akt cell survival pathway in PC12 cells: protective role in apoptosis. J Biol Chem 276, 22368–22374. [PubMed: 11294857]

Anantharam P, Kim DS, Whitley EM, Mahama B, Imerman P, Padhi P and Rumbeiha WK 2018a. Midazolam Efficacy Against Acute Hydrogen Sulfide-Induced Mortality and Neurotoxicity. Journal of medical toxicology : official journal of the American College of Medical Toxicology 14, 79–90. [PubMed: 29318511]

Anantharam P, Kim DS, Whitley EM, Mahama B, Imerman P, Padhi P and Rumbeiha WK 2018b. Midazolam Efficacy Against Acute Hydrogen Sulfide-Induced Mortality and Neurotoxicity. Journal of medical toxicology : official journal of the American College of Medical Toxicology.

Anantharam P, Whitley EM, Mahama B, Kim DS, Imerman PM, Shao D, Langley MR, Kanthasamy A and Rumbeiha WK 2017. Characterizing a mouse model for evaluation of countermeasures against hydrogen sulfide-induced neurotoxicity and neurological sequelae. Ann N Y Acad Sci 1400, 46–64. [PubMed: 28719733]

Bahar E, Kim H and Yoon H 2016. ER Stress-Mediated Signaling: Action Potential and Ca(2+) as Key Players. International journal of molecular sciences 17.

Board, U.S.C.S.a.H.I. 2004. SODIUM HYDROSULFIDE: PREVENTING HARM.

Carney PW and Jackson GD 2014. Insights into the mechanisms of absence seizure generation provided by EEG with functional MRI. Frontiers in neurology 5, 162. [PubMed: 25225491]

Cheung NS, Peng ZF, Chen MJ, Moore PK and Whiteman M 2007. Hydrogen sulfide induced neuronal death occurs via glutamate receptor and is associated with calpain activation and lysosomal rupture in mouse primary cortical neurons. Neuropharmacology 53, 505–514. [PubMed: 17692345]

Chou S, Ogden JM, Pohl HR, Scinicariello F, Ingerman L, Barber L and Citra M 2016. Toxicological profile for hydrogen sulfide and carbonyl sulfide. In: D.o.T.a.H.H. Sciences (Ed), Environmental Toxicology Branch.

Faingold CL 2002. Role of GABA abnormalities in the inferior colliculus pathophysiology - audiogenic seizures. Hear Res 168, 223–237. [PubMed: 12117523]

Garcia-Bereguiain MA, Samhan-Arias AK, Martin-Romero FJ and Gutierrez-Merino C 2008. Hydrogen sulfide raises cytosolic calcium in neurons through activation of L-type Ca2+ channels. Antioxid Redox Signal 10, 31–42. [PubMed: 17956188]

Garcia-Cairasco N, Doretto MC, Ramalho MJ, Antunes-Rodrigues J and Nonaka KO 1996. Audiogenic and audiogenic-like seizures: locus of induction and seizure severity determine postictal prolactin patterns. Pharmacology, biochemistry, and behavior 53, 503–510.

Greenberg M and Hamilton R 1998. The epidemiology of deaths related to toxic exposures in the US workplace, 1992–1996. Journal of toxicology. Clinical toxicology 5, 430.

Guidotti TL 2010. Hydrogen sulfide: advances in understanding human toxicity. International journal of toxicology 29, 569–581. [PubMed: 21076123]

Guidotti TL 2015. Hydrogen Sulfide intoxication. In: Lotti M and Bleecker ML (Eds), Handbook of clinical neurology.

Hattori K, Naguro I, Runchel C and Ichijo H 2009. The roles of ASK family proteins in stress responses and diseases. Cell communication and signaling : CCS 7, 9. [PubMed: 19389260]

Hu LF, Lu M, Tiong CX, Dawe GS, Hu G and Bian JS 2010. Neuroprotective effects of hydrogen sulfide on Parkinson's disease rat models. Aging cell 9, 135–146. [PubMed: 20041858]

Huffman RF and Henson OW Jr. 1990. The descending auditory pathway and acousticomotor systems: connections with the inferior colliculus. Brain research. Brain research reviews 15, 295–323. [PubMed: 2289088]

Jiang J, Chan A, Ali S, Saha A, Haushalter KJ, Lam WL, Glasheen M, Parker J, Brenner M, Mahon SB, Patel HH, Ambasudhan R, Lipton SA, Pilz RB and Boss GR 2016. Hydrogen Sulfide-Mechanisms of Toxicity and Development of an Antidote. Scientific reports 6, 20831. [PubMed: 26877209]

Kamiyama M, Naguro I and Ichijo H 2015. In vivo gene manipulation reveals the impact of stress-responsive MAPK pathways on tumor progression. Cancer Sci 106, 785–796. [PubMed: 25880821]

Katoh M 2012. Function and cancer genomics of FAT family genes (review). Int J Oncol 41, 1913–1918. [PubMed: 23076869]

Katsuoka F, Motohashi H, Ishii T, Aburatani H, Engel JD and Yamamoto M 2005. Genetic evidence that small maf proteins are essential for the activation of antioxidant response element-dependent genes. Mol Cell Biol 25, 8044–8051. [PubMed: 16135796]

Kilburn KH 2003. Effects of hydrogen sulfide on neurobehavioral function. Southern medical journal 96, 639–646. [PubMed: 12940311]

Kilic-Eren M, Boylu T and Tabor V 2013. Targeting PI3K/Akt represses Hypoxia inducible factor-1alpha activation and sensitizes Rhabdomyosarcoma and Ewing's sarcoma cells for apoptosis. Cancer cell international 13, 36. [PubMed: 23590596]

Kim D-S, Anantharam P, Hoffmann A, Meade ML, Grobe N, Gearhart JM, Whitley EM, Mahama B and Rumbeiha WK 2018a. Broad Spectrum Proteomics Analysis of the Inferior Colliculus following Acute Hydrogen Sulfide Exposure. Toxicology and applied pharmacology.

Kim DS, Anantharam P, Hoffmann A, Meade ML, Grobe N, Gearhart JM, Whitley EM, Mahama B and Rumbeiha WK 2018b. Broad spectrum proteomics analysis of the inferior colliculus following acute hydrogen sulfide exposure. Toxicology and applied pharmacology 355, 28–42. [PubMed: 29932956]

Kim DS, Jin H, Anantharam V, Gordon R, Kanthasamy A and Kanthasamy AG 2016. p73 gene in dopaminergic neurons is highly susceptible to manganese neurotoxicity. Neurotoxicology.

Kim DS, Jin H, Anantharam V, Gordon R, Kanthasamy A and Kanthasamy AG 2017. p73 gene in dopaminergic neurons is highly susceptible to manganese neurotoxicity. Neurotoxicology 59, 231–239. [PubMed: 27107493]

Kurokawa Y, Sekiguchi F, Kubo S, Yamasaki Y, Matsuda S, Okamoto Y, Sekimoto T, Fukatsu A, Nishikawa H, Kume T, Fukushima N, Akaike A and Kawabata A 2011. Involvement of ERK in NMDA receptor-independent cortical neurotoxicity of hydrogen sulfide. Biochem Biophys Res Commun 414, 727–732. [PubMed: 22001931]

Lavu M, Bhushan S and Lefer DJ 2011. Hydrogen sulfide-mediated cardioprotection: mechanisms and therapeutic potential. Clinical science 120, 219–229. [PubMed: 21126235]

Lee ER, Kim JY, Kang YJ, Ahn JY, Kim JH, Kim BW, Choi HY, Jeong MY and Cho SG 2006. Interplay between PI3K/Akt and MAPK signaling pathways in DNA-damaging drug-induced apoptosis. Biochim Biophys Acta 1763, 958–968. [PubMed: 16905201]

Lee ZW, Zhou J, Chen CS, Zhao Y, Tan CH, Li L, Moore PK and Deng LW 2011. The slow-releasing hydrogen sulfide donor, GYY4137, exhibits novel anti-cancer effects in vitro and in vivo. miR oxidative stress 6, e21077.

Los M, Maddika S, Erb B and Schulze-Osthoff K 2009. Switching Akt: from survival signaling to deadly response. BioEssays : news and reviews in molecular, cellular and developmental biology 31, 492–495.

Mailloux RJ and Harper ME 2011. Uncoupling proteins and the control of mitochondrial reactive oxygen species production. Free Radic Biol Med 51, 1106–1115. [PubMed: 21762777]

Matsuo F, Cummins JW and Anderson RE 1979. Neurological sequelae of massive hydrogen sulfide inhalation. Archives of neurology 36, 451–452.

Motloch LJ, Larbig R, Gebing T, Reda S, Schwaiger A, Leitner J, Wolny M, Eckardt L and Hoppe UC 2016. By Regulating Mitochondrial Ca2+-Uptake UCP2 Modulates Intracellular Ca2+. miR oxidative stress 11, e0148359.

National Institute of Allergy and Infectious Diseases. 2007. NIH Strategic Plan and Research Agenda for Medical Countermeasures Against Chemical Threats. In: U.S.D.o.H.a.H. Services (Ed), National Institutes of Health.

Ng PC, Hendry-Hofer TB, Witeof AE, Brenner M, Mahon SB, Boss GR, Haouzi P and Bebarta VS 2019. Hydrogen Sulfide Toxicity: Mechanism of Action, Clinical Presentation, and Countermeasure Development. Journal of medical toxicology : official journal of the American College of Medical Toxicology.

Olas B 2014. Hydrogen sulfide in hemostasis: friend or foe? Chem Biol Interact 217, 49–56. [PubMed: 24746521]

Pappalardo F, Russo G, Candido S, Pennisi M, Cavalieri S, Motta S, McCubrey JA, Nicoletti F and Libra M 2016. Computational Modeling of PI3K/AKT and MAPK Signaling Pathways in Melanoma Cancer. miR oxidative stress 11, e0152104.

Parra O, Monso E, Gallego M and Morera J 1991. Inhalation of hydrogen sulphide: a case of subacute manifestations and long term sequelae. British journal of industrial medicine 48, 286–287. [PubMed: 2025598]

Rumbeiha W, Whitley E, Anantharam P, Kim DS and Kanthasamy A 2016. Acute hydrogen sulfide-induced neuropathology and neurological sequelae: challenges for translational neuroprotective research. Ann N Y Acad Sci 1378, 5–16. [PubMed: 27442775]

Sams RN, Carver HW 2nd, Catanese C and Gilson T 2013. Suicide with hydrogen sulfide. The American journal of forensic medicine and pathology 34, 81–82. [PubMed: 23574866]

Sarkar S, Malovic E, Harischandra DS, Ngwa HA, Ghosh A, Hogan C, Rokad D, Zenitsky G, Jin H, Anantharam V, Kanthasamy AG and Kanthasamy A 2018a. Manganese exposure induces neuroinflammation by impairing mitochondrial dynamics in astrocytes. Neurotoxicology 64, 204–218. [PubMed: 28539244]

Sarkar S, Malovic E, Sarda D, Lawana V, Rokad D, Jin H, Anantharam V, Kanthasamy A and Kanthasamy AG 2018b. Characterization and comparative analysis of a new mouse microglial cell model for studying neuroinflammatory mechanisms during neurotoxic insults. Neurotoxicology 67, 129–140. [PubMed: 29775624]

Srinivasan S and Avadhani NG 2012. Cytochrome c oxidase dysfunction in oxidative stress. Free Radic Biol Med 53, 1252–1263. [PubMed: 22841758]

Tan BH, Wong PT and Bian JS 2010. Hydrogen sulfide: a novel signaling molecule in the central nervous system. Neurochem Int 56, 3–10. [PubMed: 19703504]

Trapnell C, Roberts A, Goff L, Pertea G, Kim D, Kelley DR, Pimentel H, Salzberg SL, Rinn JL and Pachter L 2012. Differential gene and transcript expression analysis of RNA-seq experiments with TopHat and Cufflinks. Nature protocols 7, 562–578. [PubMed: 22383036]

Truong DH, Eghbal MA, Hindmarsh W, Roth SH and O'Brien PJ 2006. Molecular mechanisms of hydrogen sulfide toxicity. Drug metabolism reviews 38, 733–744. [PubMed: 17145698]

Tvedt B, Edland A, Skyberg K and Forberg O 1991a. Delayed neuropsychiatric sequelae after acute hydrogen sulfide poisoning: affection of motor function, memory, vision and hearing. Acta neurologica Scandinavica 84, 348–351. [PubMed: 1772008]

Tvedt B, Skyberg K, Aaserud O, Hobbesland A and Mathiesen T 1991b. Brain damage caused by hydrogen sulfide: a follow-up study of six patients. American journal of industrial medicine 20, 91–101. [PubMed: 1867221]

Department of Health US and Human Services A 2014. Draft Toxicological Profile for Hydrogen Sulfide and Carbonyl Sulfide. ATSDR, Atlanta, GA.

Wang J, Lee J, Liem D and Ping P 2017. HSPA5 Gene encoding Hsp70 chaperone BiP in the endoplasmic reticulum. Gene 618, 14–23. [PubMed: 28286085]

Wasch HH, Estrin WJ, Yip P, Bowler R and Cone JE 1989. Prolongation of the P-300 latency associated with hydrogen sulfide exposure. Archives of neurology 46, 902–904. [PubMed: 2757531]

Yong QC, Choo CH, Tan BH, Low CM and Bian JS 2010. Effect of hydrogen sulfide on intracellular calcium homeostasis in neuronal cells. Neurochem Int 56, 508–515. [PubMed: 20026367]

Highlights

- Transcriptomic profiling analyses following acute exposure to H_2S were performed
- Multiple signaling pathways were dysregulated following H_2S exposure
- PI3K/Akt and MAPK signaling pathways were activated after H_2S exposure
- MRI scan analysis revealed lesions in the IC and TH following H_2S exposure
- Acute H_2S exposure induced a neuroinflammatory response

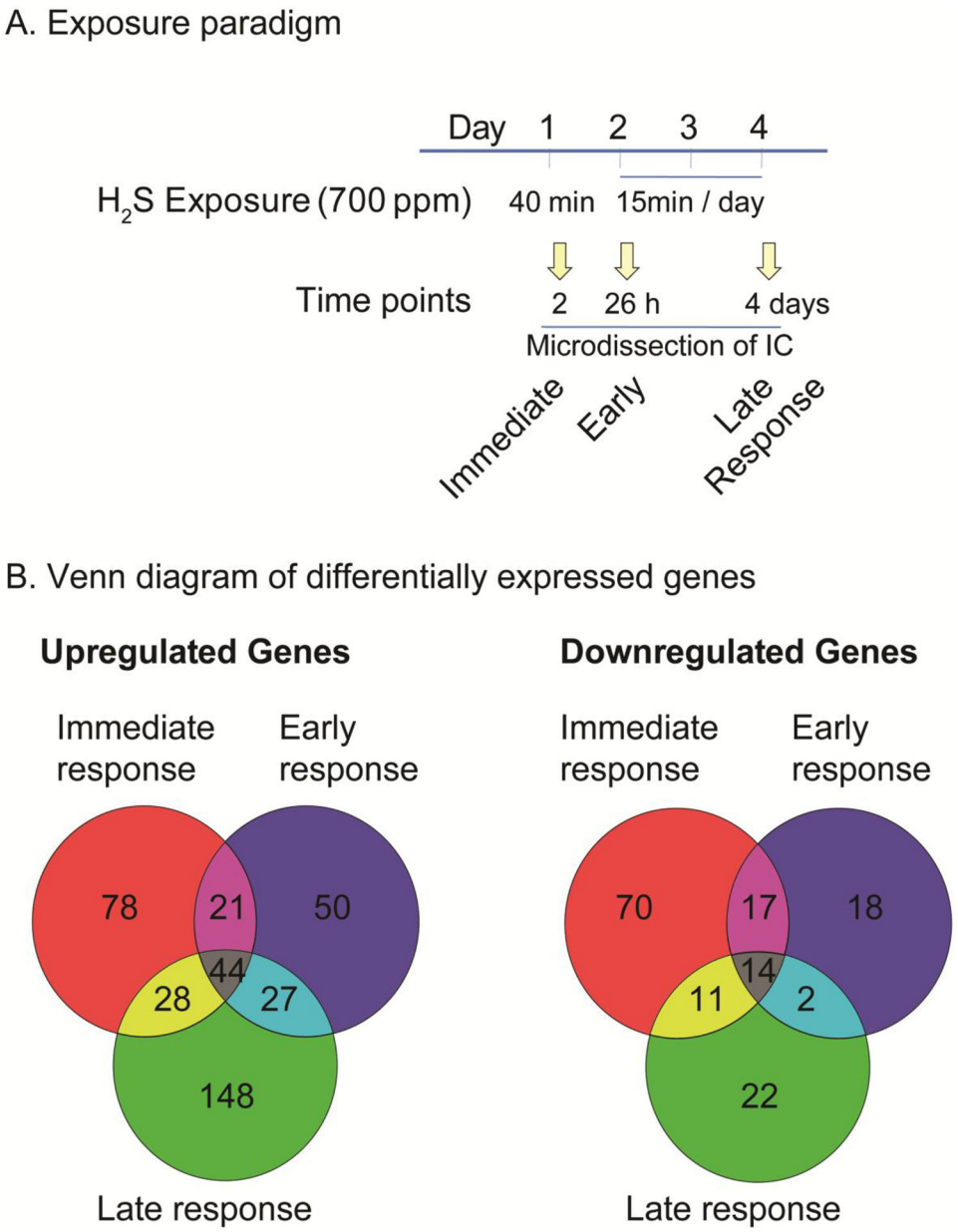

Figure 1.

Hydrogen sulfide exposure paradigm and Venn diagram of differentially expressed genes (DEGs) after acute exposure to H_2S in the IC.

C57 black mice were exposed via whole body exposure to 700 ppm H_2S. A scheme of exposure paradigm was shown (A). The microdissected IC was used for transcriptomic analysis. The numbers of DEGs at immediate, early, and late response to H_2S exposure in the IC are shown in Venn diagrams (B).

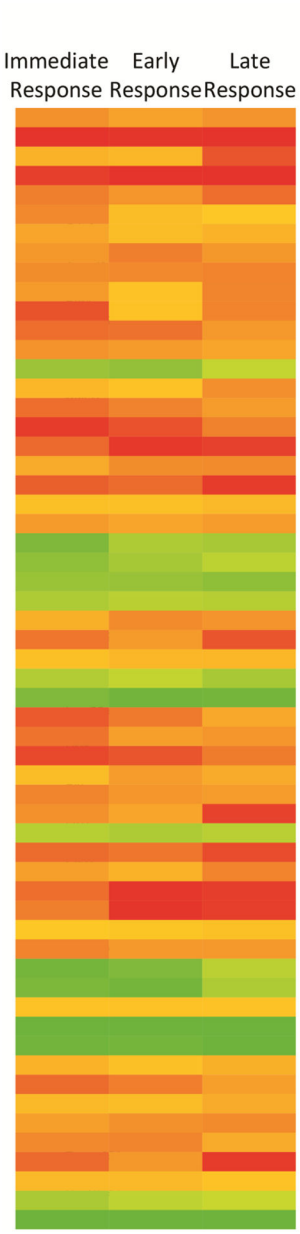

symbol	name	GOBP (final)
Ada	Adenosine Deaminase	Inflammatory response signaling
Ccl2	chemokine (C-C motif) ligand 2	Inflammatory response signaling
Cebpd	CCAAT/enhancer binding protein (C/EBP), delta	Inflammatory response signaling
Crtam	Cytotoxic And Regulatory T Cell Molecule	Inflammatory response signaling
Ctla2a	cytotoxic T lymphocyte-associated protein 2 alpha	Inflammatory response signaling
Nfkbia	NFKB Inhibitor Alpha	Inflammatory response signaling
Tinagl1	Tubulointerstitial Nephritis Antigen Like 1	Inflammatory response signaling
Zfp36	ZFP36 Ring Finger Protein	Inflammatory response signaling
Egr4	early growth response 4	Cellular stress response signaling
Gadd45g	Growth Arrest And DNA Damage Inducible Gamma	Cellular stress response signaling
Maff	MAF BZIP Transcription Factor F	Cellular stress response signaling
Sgk1	Serum/Glucocorticoid Regulated Kinase 1	Cellular stress response signaling
Txnip	Thioredoxin Interacting Protein	Cellular stress response signaling
Sdf2l1	Stromal Cell Derived Factor 2 Like 1	Cellular stress response signaling
Cd93	CD93 Molecule	Cell survival / death signaling
Cdkn1a	Cyclin-Dependent Kinase Inhibitor 1A	Cell survival / death signaling
Cep131	centrosomal protein 131kDa	Cell survival / death signaling
Fat2	FAT atypical cadherin 2	Cell survival / death signaling
Fos	FBJ Murine Osteosarcoma Viral Oncogene Homolog	Cell survival / death signaling
Fosb	FBJ Murine Osteosarcoma Viral Oncogene Homolog B	Cell survival / death signaling
Pglyrp1	Peptidoglycan Recognition Protein 1	Cell survival / death signaling
Ror1	Receptor Tyrosine Kinase Like Orphan Receptor 1	Cell survival / death signaling
Depdc7	DEP Domain Containing 7	Cell survival / death signaling
Nkx2-9	NK2 homeobox 9	Cell survival / death signaling
Lbr	Lamin B Receptor	Genome sability
Rint1	RAD50 Interactor 1	Genome sability
Neurod2	Neuronal Differentiation 2	Calciumsignaling
P2ry2	Purinergic Receptor P2Y2	Calciumsignaling
Ucp2	Uncoupling Protein 2	Hypoxic signaling
Erbb3	Erb-B2 Receptor Tyrosine Kinase 3	Hypoxic signaling
Fam60a	family with sequence similarity 60, member A	Hypoxic signaling
Apold1	Apolipoprotein L Domain Containing 1	Angiogenesis
Ctgf	Connective Tissue Growth Factor	Angiogenesis
Cyr61	cysteine-rich, angiogenic inducer, 61	Angiogenesis
Eln	Elastin	Angiogenesis
Lox	Lysyl Oxidase	Angiogenesis
Lrg1	leucine-rich alpha-2-glycoprotein 1	Angiogenesis
P4ha1	Prolyl 4-Hydroxylase Subunit Alpha 1	Angiogenesis
Edn1	Endothelin 1	Hemorrage
Serpine1	Serpin Family E Member 1	Hemorrage
Cbln3	cerebellin 3 precursor	Neurotransmitter signaling
Gabra6	gamma-aminobutyric acid (GABA) A receptor, alpha 6	Neurotransmitter signaling
Gabrd	Gamma-Aminobutyric Acid Type A Receptor Delta Subunit	Neurotransmitter signaling
Slc17a7	Solute Carrier Family 17 Member 7	Neurotransmitter signaling
Dbh	dopamine beta-hydroxylase	Neurotransmitter signaling
Slc6a2	Solute Carrier Family 6 Member 2	Neurotransmitter signaling
Cartpt	CART Prepropeptide	Hormone
Gh	Growth Hormone	Hormone
Rln3	Relaxin 3	Hormone
Opalin	Oligodendrocytic Myelin Paranodal And Inner Loop Protein	Myelination
Arl4d	ADP Ribosylation Factor Like GTPase 4D	Intracellular trafficking
Cyp1b1	Cytochrome P450 Family 1 Subfamily B Member 1	Drug metabolism
Stra6	Stimulated By Retinoic Acid 6	Transport of biomolecules
Arrdc2	Arrestin Domain Containing 2	Unknown
Tmem252	Transmembrane Protein 252	Unknown
Tmem81	Transmembrane Protein 81	Unknown
Gm42547		Unknown
Rnf225	Ring Finger Protein 225	Unknown

Figure 2.

Heatmaps of DEGs in the IC after acute exposure to H_2S.

RNA-seq analysis of gene expression changes in the IC after H_2S exposure. Expression of DEGs at immediate, early, and late response to H_2S exposure are shown in heat map view. Genes with higher expression levels are shown in red, whereas genes with lower expression levels are shown in green. Gene names and gene ontology of biological pathways are shown in the right panel.

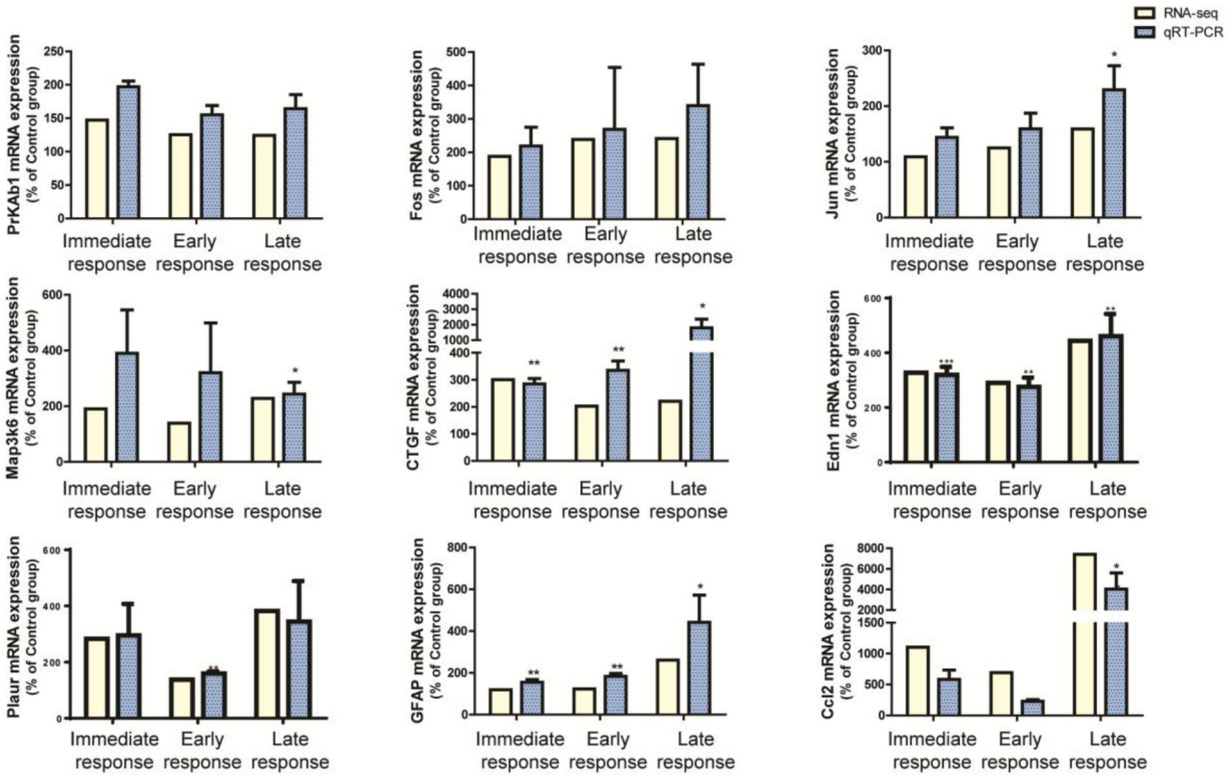

Figure 3.

RNAseq analysis of the IC of H_2S exposed mice were validated with quantitative real-time PCR.

Expression profiles of RNAseq analyses in the IC were validated with the analyses of quantitative real-time PCR. Genes that were differentially expressed in common throughout H_2S exposure were selected for this analysis. Expressions of genes were measured by quantitative real-time PCR (n>3) and compared to gene expression profiles of RNAseq analyses in the IC. Values of quantitative real-time PCR were normalized to Gapdh expression. Significant difference were determined by t-test by comparison to the breathing air control group and were indicated with *($p<0.05$) or **($p<0.01$).

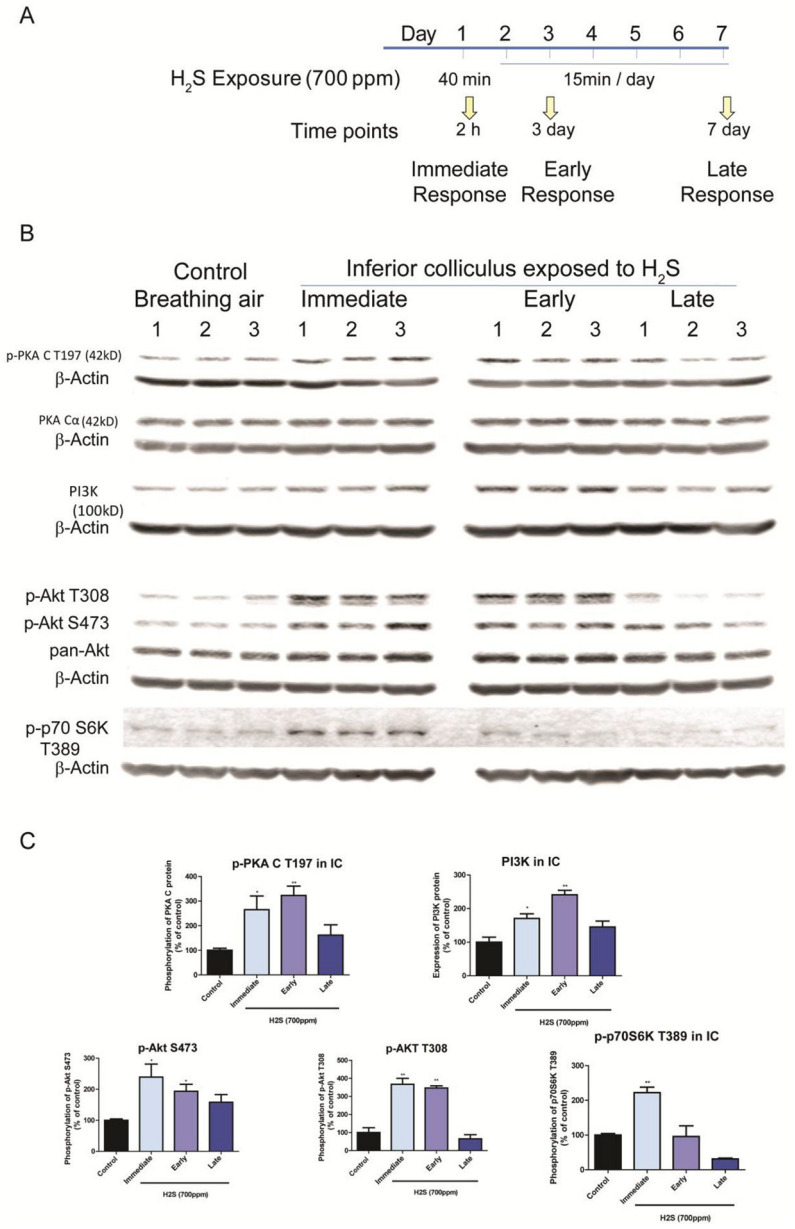

Figure 4.

H_2S exposure activated the PI3K/Akt signaling pathway

Activation of PI3K/Akt signaling pathways in the IC after H_2S exposure was measured by Western blotting analyses. A, Phosphorylation of AKT at both S474 and T308 was increased at the immediate and early response time points following H_2S exposure compared to the breathing air control group. Expression of PI3K was also upregulated at the immediate and early response times following H_2S exposure compared to the breathing air control group. Phosphorylation of PKA C at T197 was also increased at the immediate and early response times points H_2S exposure. Phosphorylation of p-70S6k at T389 was increased at the immediate response to H_2S exposure. B, band intensities of Western blotting in A were measured and visualized in graph view. Significant differences were determined by t-test

with comparison to the breathing air control group and were indicated with *($p<0.05$) or **($p<0.01$).

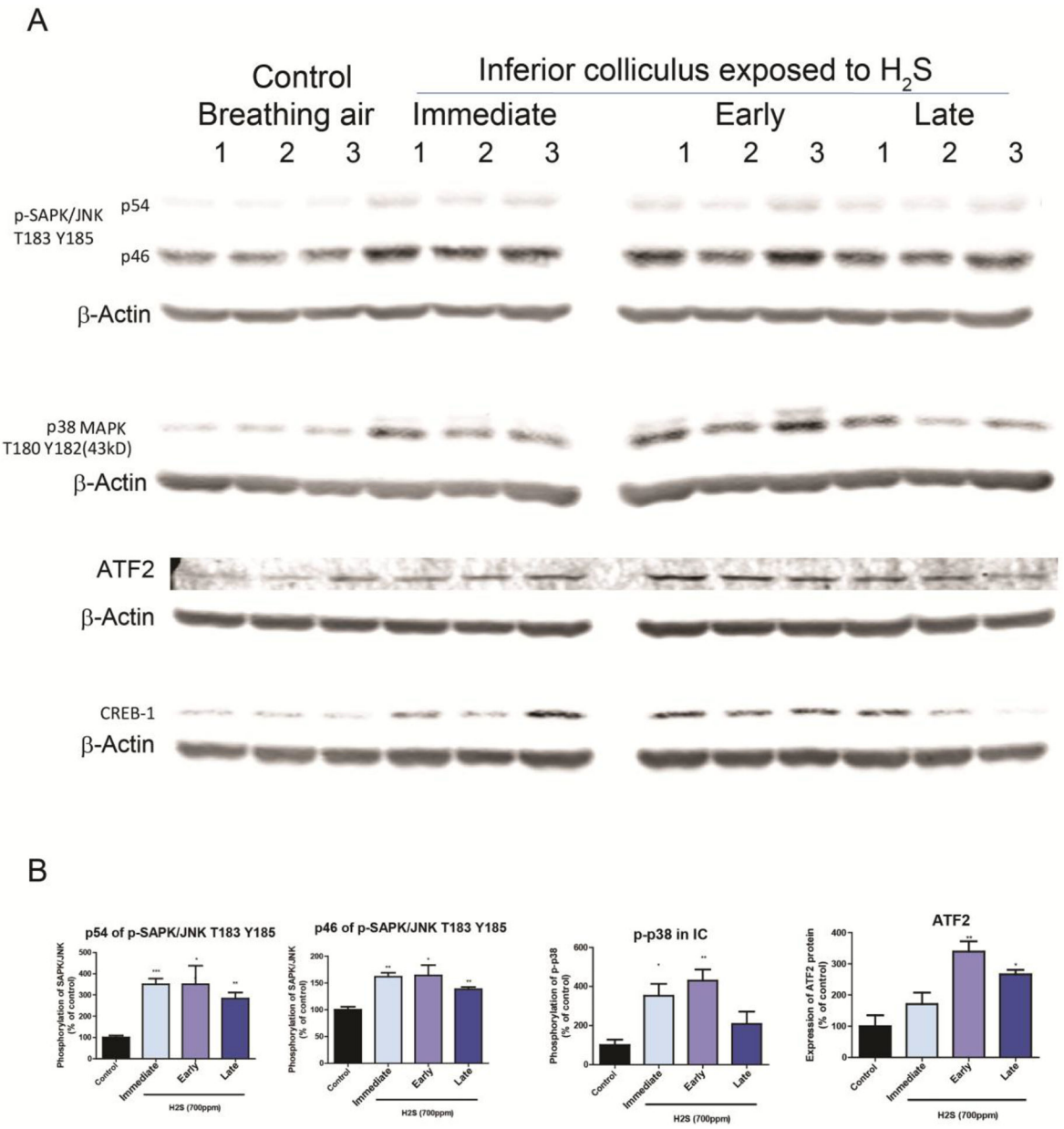

Figure 5.

H_2S exposure activated the MAPK signaling pathway in the IC

Activation of the MAPK signaling pathways in the IC after H_2S exposure was measured with Western blotting analyses. A, Phosphorylation of SAPK/JNK at T183/Y185 was increased after H_2S exposure compared to the breathing air control group. Phosphorylation of p38 was increased at the immediate and early response times following acute H_2S exposure. Expression of ATF2 was upregulated at early and late response to H_2S exposure compared to the breathing air control group. B, band intensities of Western blotting in A were measured and visualized in graph view. Significant differences were determined by t-test with comparison to breathing air control group and were indicated with *($p<0.05$) or **($p<0.01$).

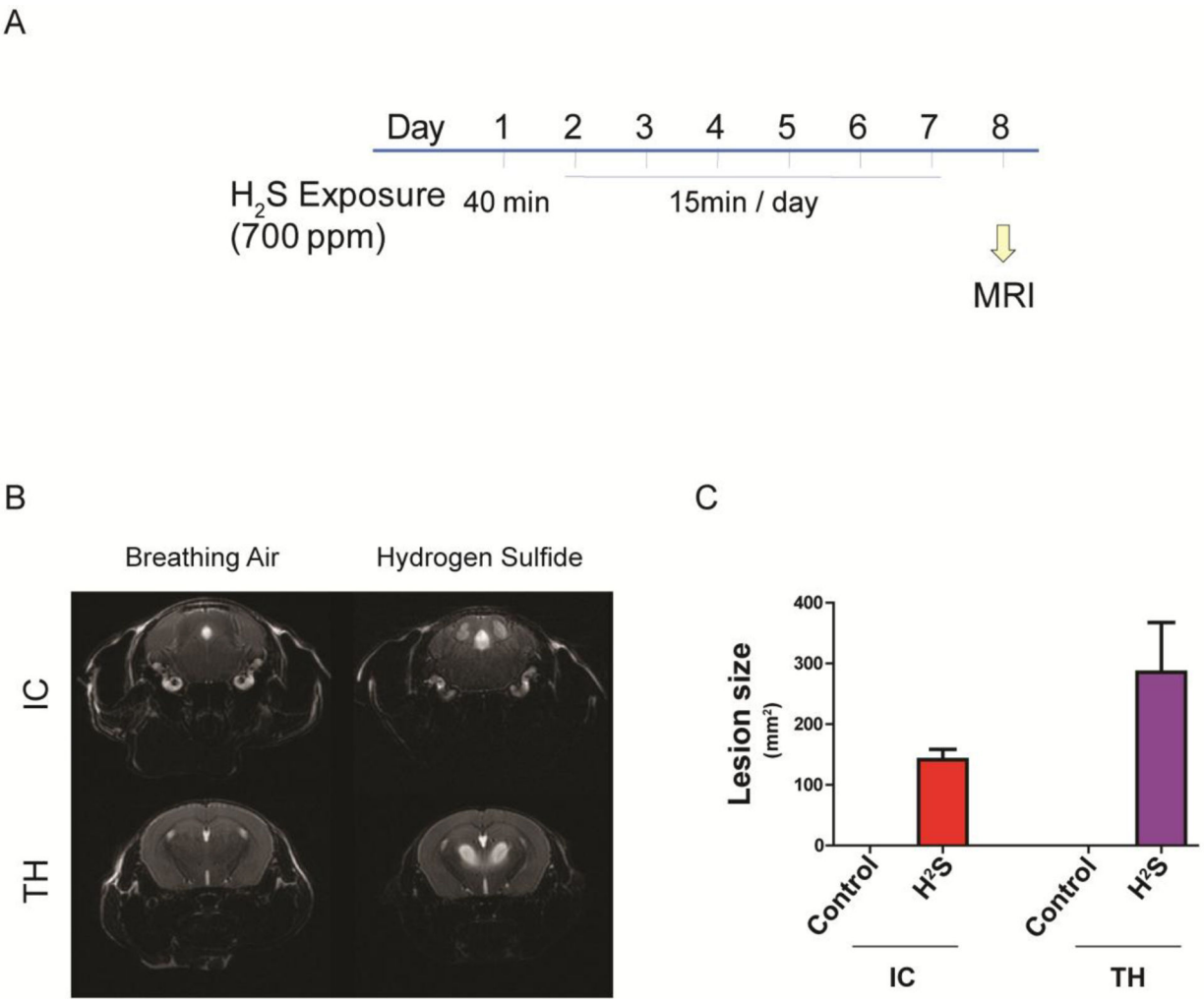

Figure 6.

Acute exposure to H_2S induced brain lesion in IC and TH

Mice were acutely exposed to H_2S daily for 7 days, followed by scanning T2-weighted MRI. A scheme of the exposure paradigm is shown (A). The MRI images of the IC and TH regions are shown (B). Hydrogen sulfide exposure lesions in IC and TH were measured and visualized in graph view (C).

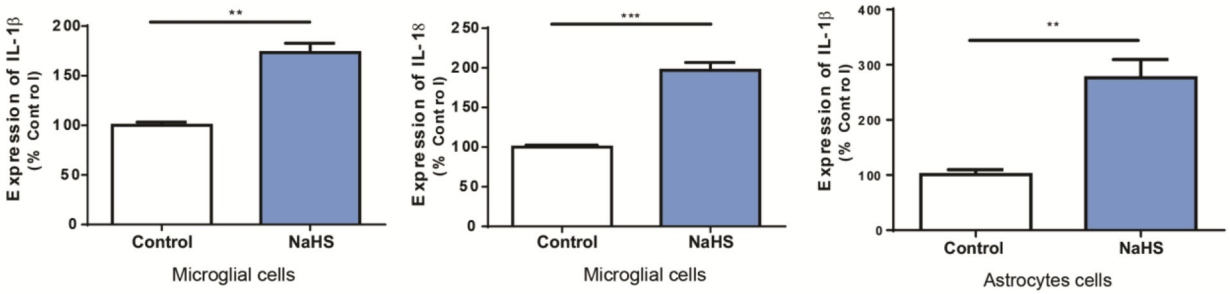

Figure 7.

Microglia and astrocytes release cytokines following H_2S exposure

Mouse microglial cells and human astrocyte cells were exposed to 1mM of sodium hydrosulfide (NaHS) for 6 h. Expression of IL-1β and IL-18 was examined using quantitative RT-PCR. Gene expression was compared to control group. Gapdh was used as internal reference gene. Significant differences were determined by t-test with comparison to breathing air control group and were indicated with **($p<0.01$) or ***($p<0.001$).

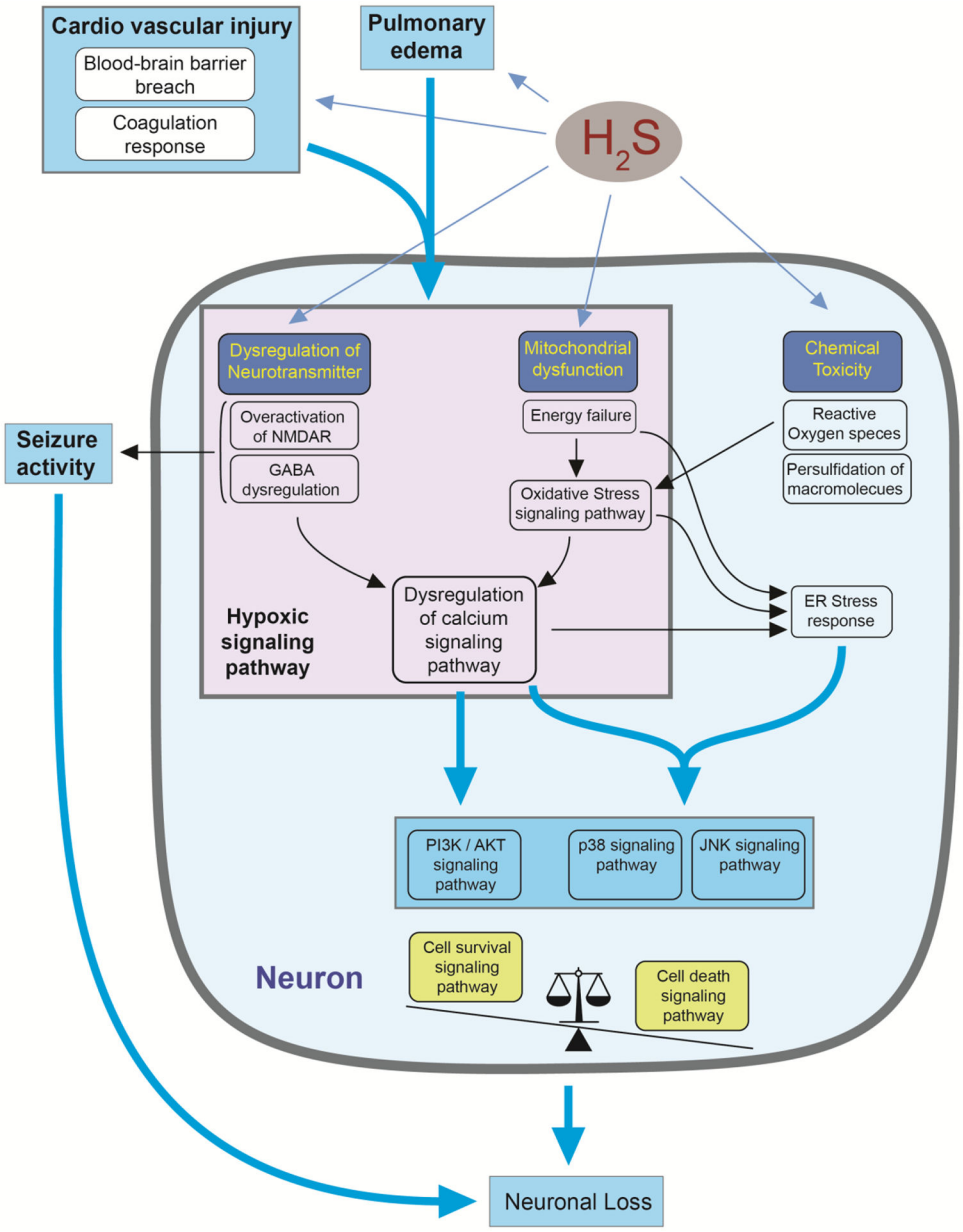

Figure 8.

A hypothetical diagram summarizing the pathways leading to H_2S-induced neuronal cell death. Hydrogen sulfide exposure induces dysregulation of multiple biological pathways leading to neuronal loss in the IC. Pulmonary edema and cardiovascular injury may reduce supply of oxygen, which may play a role in inducing the hypoxic signaling pathway. In addition, dysregulation of neurotransmitters such as NMDA and GABA and mitochondrial dysfunction may induce hypoxic signaling pathway, which may lead to calcium dysregulation and cell survival and death signaling pathways. Mitochondrial dysfunction and dysregulated calcium signaling may induce ER stress response and cell death signaling pathway. When cell death signaling pathway overcomes survival signaling pathway,

neuronal loss may occur. Seizure activity derived from dysregulation of neurotransmitter system may further affect on neuronal loss.

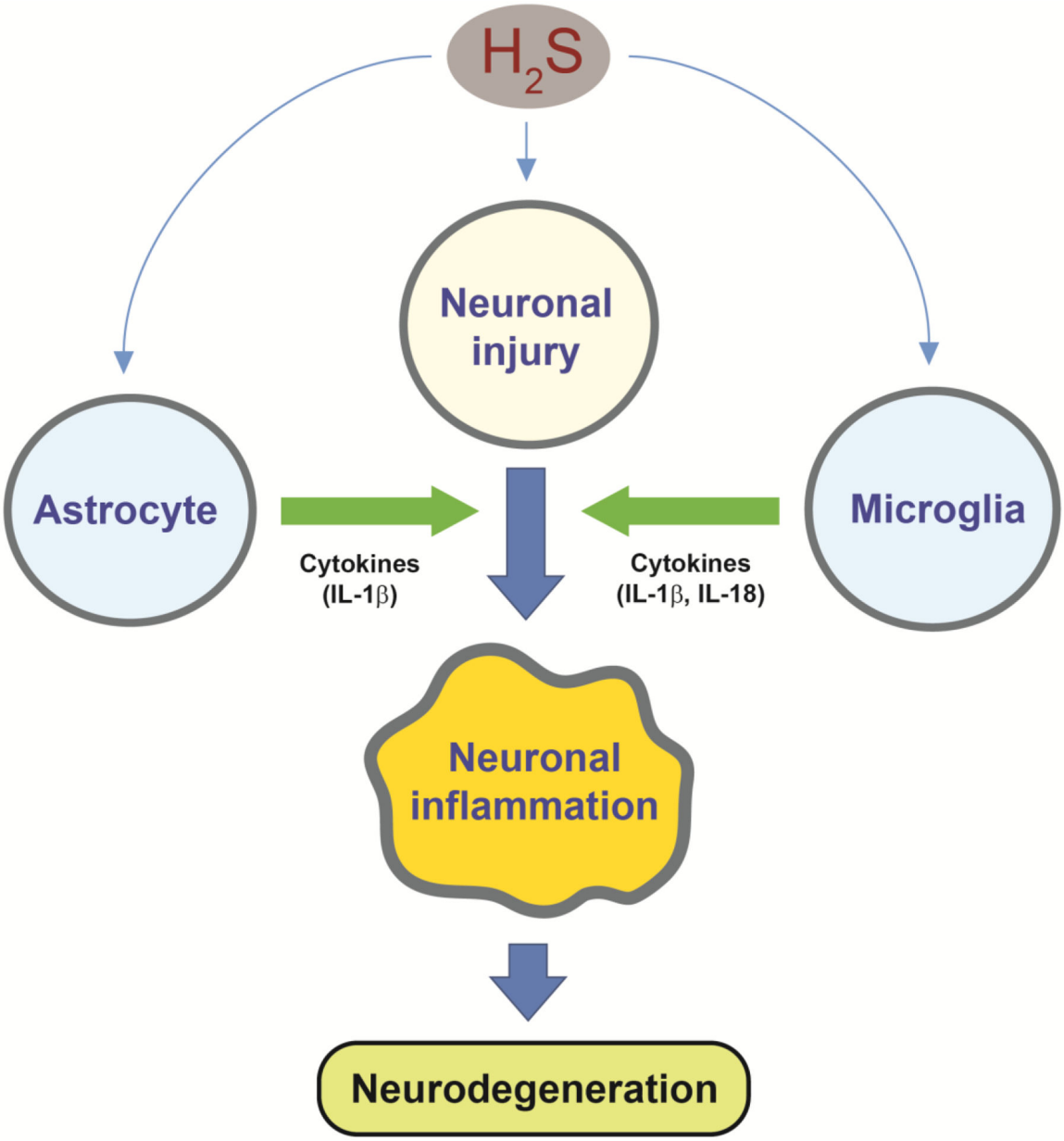

Figure 9.

H_2S exposure activates astrocyte and microglia in addition to neuronal injury. Pro-inflammatory cytokines such as IL-1β and IL-18 from astrocytes and microglia may accelerate neuronal inflammation leading to massive neurodegeneration in IC.

Table 1.

The top 10 dysregulated biological pathways at immediate (2 h), early (26 h) and late (day 4) response in IC following acute H_2S exposure.

Exposure	Pathway	pValue	z-Score
Immediate response	Unfolded protein response	1.05E-06	
Immediate response	Catecholamine Biosynthesis	6.72E-05	
Immediate response	Coagulation System	2.48E-04	
Immediate response	GADD45 Signaling	1.25E-03	
Immediate response	Dopamine Receptor Signaling	3.73E-03	
Immediate response	NRF2-mediated Oxidative Stress Response	4.51E-03	1.342
Immediate response	GABA Receptor Signaling	7.61E-03	1
Immediate response	Death Receptor Signaling	9.78E-03	0.378
Immediate response	eNOS Signaling	1.95E-02	0.707
Immediate response	p53 Signaling	2.51E-02	2
Early response	Unfolded protein response	2.05E-07	
Early response	NRF2-mediated Oxidative Stress Response	8.26E-05	0.447
Early response	Hypoxia Signaling in the Cardiovascular System	8.94E-05	1.633
Early response	Coagulation System	2.44E-04	−0.447
Early response	Endoplasmic Reticulum Stress Pathway	3.34E-04	
Early response	Acute Phase Response Signaling	4.74E-04	2.646
Early response	PI3K Signaling in B Lymphocytes	5.08E-03	0.816
Early response	Calcium Signaling	9.02E-03	−0.447
Early response	IL-6 Signaling	1.80E-02	0.816
Early response	HMGB1 Signaling	2.20E-02	1.342
Late response	Agranulocyte Adhesion and Diapedesis	1.55E-10	
Late response	Granulocyte Adhesion and Diapedesis	1.08E-08	
Late response	Acute Phase Response Signaling	1.67E-07	2.887
Late response	HMGB1 Signaling	2.00E-07	2.673
Late response	IL-10 Signaling	2.18E-07	
Late response	Coagulation System	8.45E-06	−1.134
Late response	phagosome formation	1.38E-05	
Late response	IL-6 Signaling	1.01E-04	1.897
Late response	JAK/Stat Signaling	4.32E-04	0.707
Late response	PPAR Signaling	9.24E-04	−2.828

Dysregulated biological pathways were analyzed for immediate, early, and late response to H_2S exposure. The top 10 dysregulated biological pathways were measured by statistical analyses and are listed. Degree of activating biological pathways is shown by the z-Score. Higher value of z-Score indicates activation of biological pathways, whereas lower value of z-Score for inactivation of biological pathways.

Table 2.

Potential upstream regulators in the IC responding to acute H_2S exposure.

Exposure	Name	p-value	z-score
Immediate response	TNF	3.96e-23	2.178
Immediate response	LPS	5.94e-20	3.084
Immediate response	PDGF BB	2.36e-19	3.645
Immediate response	CREB1	6.95e-19	3.669
Immediate response	PKC	6.86e-18	3.69
Immediate response	TGF-β1	1.94e-17	3.8
Immediate response	FGF2	6.87e-17	1.562
Immediate response	EGFR	8.33e-17	1.339
Immediate response	TP53	5.13e-15	3.049
Immediate response	IL 1b	7.39e-15	3.299
Early response	LPS	6.19e-21	2.849
Early response	IL-1β	7.55e-20	2.736
Early response	CREB1	5.86e-19	2.722
Early response	D-glucose	6.26e-18	3.197
Early response	IGF1	9.02e-18	3.395
Early response	TGF-β1	9.27e-18	3.933
Early response	PDGF BB	2.75e-17	3.758
Early response	TNF	7.54e-16	1.704
Early response	TP53	1.42e-15	2.525
Early response	Insulin	7.25e-15	2.602
Late response	LPS	7.73e-64	8.368
Late response	TNF	7.73e-55	5.13
Late response	TGF-β1	1.47e-47	5.157
Late response	IFN-γ	3.15e-45	7.274
Late response	IL-1β	3.25e-42	5.658
Late response	STAT3	2.0e-40	2.884
Late response	IL4	1.63e-36	3.725
Late response	IL6	1.29e-32	5.893
Late response	U0126	2.78e-30	−5.359
Late response	PDGF BB	4.26e-28	5.277

Potential upstream regulators were analyzed at immediate (2 h), early (26 h), and late response (day 4) to acute H_2S exposure. The top 10 potential upstream regulators were statistically analyzed and are listed. Degree of activating biological pathways is shown by z-Score. Higher value of z-Score indicates activation of potential upstream regulator, whereas lower value of z-Score for inactivation of potential upstream regulator.